Hindawi
Mobile Information Systems
Volume 2022, Article ID 9548552, 11 pages
https://doi.org/10.1155/2022/9548552

Research Article

Remote Sensing Recognition and Classification of Forest Vegetation Based on Image Feature Depth Learning

Gang Jiang[1,2,3] **and Quanshun Zheng**[4]

[1]*Key Laboratory of Tibetan Plateau Land Surface Processes and Ecological Conservation (Ministry of Education), Qinghai Normal University, Xining 810008, Qinghai, China*
[2]*Qinghai Province Key Laboratory of Physical Geography and Environmental Process, College of Geographical Science, Qinghai Normal University, Xining 810008, Qinghai, China*
[3]*State Key Laboratory of Remote Sensing Science, Jointly Sponsored By Beijing Normal University and Aerospace Information Research, Institute of Chinese Academy of Sciences, Faculty of Geographical Science, Beijing Normal University, Beijing 100875, Beijing, China*
[4]*Maintenance Company of Qinghai Electric Power Company of State Grid, Xining 810000, Qinghai, China*

Correspondence should be addressed to Gang Jiang; jianggang21@qhnu.edu.cn

Received 14 March 2022; Revised 9 April 2022; Accepted 31 May 2022; Published 28 June 2022

Academic Editor: Fusheng Zhu

In order to study the remote sensing recognition and classification of forest vegetation based on image feature depth learning, this paper presents a deep learning method using classical algorithms such as the maximum class method and maximum entropy method, as well as the FRFCM algorithm and convolutional neural network. In this method, SVM is used to train, classify, and recognize the color information of a high-resolution remote sensing image, remove the nongreen background of the classified image, and finally convert it to HSI space for morphological opening and closing reconstruction, so as to obtain the final extraction target. Then, a visual interface is designed to facilitate operation, which can compare the forest vegetation extraction results and operation processing time under different algorithms, so as to realize the rapid and accurate monitoring of karst forest vegetation change with remote sensing big data. The algorithm research shows that the overall accuracy of multifeature ant colony intelligent classification based on vegetation zoning is 88.85%, Kappa = 0.86, which is better than the traditional remote sensing image classification method, and provides an effective method for land use land cover remote sensing information extraction in large-scale complex terrain areas. In this way, the error extraction and missing extraction can be reduced in the extraction results of forest vegetation area in remote sensing images, and the experimental extraction results will be further close to the optimal segmentation effect.

1. Introduction

As a special type of image taken by satellites and other aircraft, high-resolution remote sensing image has important value and position in military and civil fields. Forest vegetation is one of the main factors affecting the Earth's ecological environment. Forestry departments need to use forest surveys to obtain basic data such as the quantity and quality of forest vegetation and dynamically monitor changes in forest vegetation. Deep learning is a machine learning method emerging in recent years. It can automatically learn the deep essential characteristics and laws of a large number of historical data, so as to identify, judge, or predict the future of new data, and improve the accuracy of classification and recognition to a certain extent. Therefore, using the depth learning method to classify remote sensing images is of great significance. Remote sensing technology provides the Ministry of forestry with the only effective and economic method to quickly monitor the current situation and dynamic change of large-area forest vegetation. In

recent years, it has been widely used in forest investigation, especially the emergence and application of high-resolution remote sensing images such as quick bird with submeter spatial resolution, which makes it possible to investigate forest vegetation carefully. Remote sensing image contains rich feature information, which is the most intuitive expression of the overall appearance of features. Feature extraction of remote sensing image is the most basic operation to study target features and obtain feature information (Figure 1). The research on remote sensing image classification and recognition not only has scientific theoretical significance but also has practical significance [1].

2. Literature Review

Jaime and others proposed using the feature training classifier of image pixels in remote sensing images for target extraction. This method has great advantages in controlling the statistics of color images and can bypass a large number of tasks to find the optimal threshold. This method is used for image segmentation [2, 3]. Meng and others obtained a land-use type map with an accuracy of 98.2% by combining supervised and unsupervised classification methods in the study of land use classification and obtained better results than using these two methods independently [4]. Shakya, A. and others used the decision tree method to classify land cover and compared it with other methods. The results show that the decision tree method improves the classification accuracy by 3%–6% [5]. Cao and others applied the fuzzy classification method to the study of impervious surface performance and compared it with the LSMA method. The results show that the fuzzy classification method is better than the LSMA method in any season, and the performance of the fuzzy classification method is better in both high-density residential areas and low-density residential areas [6]. Gao and others studied the land use types of Xinqiao town based on quick bird images. Due to the shortcomings of visual interpretation, many scholars have gradually sought other effective image classification methods [7]. Chen and others compared the K-means clustering method based on three similarity measures on virus remote sensing data. The experiment shows that the K-means clustering method based on Euclidean distance has the best accuracy and efficiency [8]. Wang and others used BP neural network to classify high-resolution remote sensing images. Through experiments, it is found that the adaptive dynamic system classification of the BP neural network has a better effect on land cover classification than other commonly used classifications [9]. Zhao and others proposed a method for texture segmentation of forest vegetation in remote sensing images based on the visual attention mechanism. Firstly, the crown shape and structure inside the image are regarded as visual attention targets, and then, the texture is enhanced. The forest vegetation area is segmented through the improved region growth method [10]. Khelifi and others believe that, at present, there are many kinds of classification algorithms for remote sensing images, such as ISODATA, K-means, minimum distance, maximum likelihood, and other algorithms. For this reason, people divide the above classification algorithms into supervised and unsupervised, parametric, and nonparametric, based on different principles, and focus on the above classification algorithms based on several categories such as pixels, subpixels, and objects. Due to the influence of many external factors, such as the complex surface environment, the screening of remote sensing images, the quality of image preprocessing, and the selection of classification methods, there is still much room for improvement [11].

3. Image Feature Extraction

Image feature extraction is the use of a computer to extract the relevant information contained in the image. In this process, it is judged that the features contained in the pixels in the image are suitable for classification, and the feature extraction method is used under certain requirements. Image feature extraction is to use the computer to extract the relevant information contained in the image. In this process, it is judged that the features contained in the pixels in the image are suitable for classifying them, and the method of feature extraction is used when certain requirements are met. The original image is classified, and there are points, curves, and connected blocks in the classified regions. The original image is classified, and there are points, curves, and areas connected into blocks in the areas of each category after classification. If the algorithm used is used to calculate some characteristic parts of the image data, then the characteristic extraction itself can be attributed to the image processing algorithm used. Image segmentation plays an indispensable role in the entire image research field (as shown in Figure 2). The work quality of this step will have a very intuitive impact on the entire image processing process.

For a long period of time, the threshold-based segmentation method has always been the basic content of image segmentation research, which is convenient to use and has obvious effects. The use process is that the gray histogram information of the obtained remote sensing image is first used for calculation and analysis, to obtain the threshold value, and then, the image is divided into different marked blocks by the threshold value, and formula (1) is used to express. It can be seen that finding the optimal threshold has become the key to research. Generally, the algorithm is divided into the global threshold method and local threshold method in the research. The global threshold method is to find the optimal threshold according to all gray information in the image to divide all data in the image. When double peaks are observed from the gray histogram of the experimental data, the lowest point of the curve between the double peaks can be regarded as the threshold, and the target area can be distinguished from the irrelevant area [12] as shown in Figure 3.

$$g(x,y) = \begin{cases} 1 & g(x,y) < Th \\ 0 & f(x,y) < Th \end{cases}, \tag{1}$$

If the size of the image is set to $M \times N$, the number of pixels can use H, indicating that G is used to represent the gray level of the image. When i is used to represent the gray

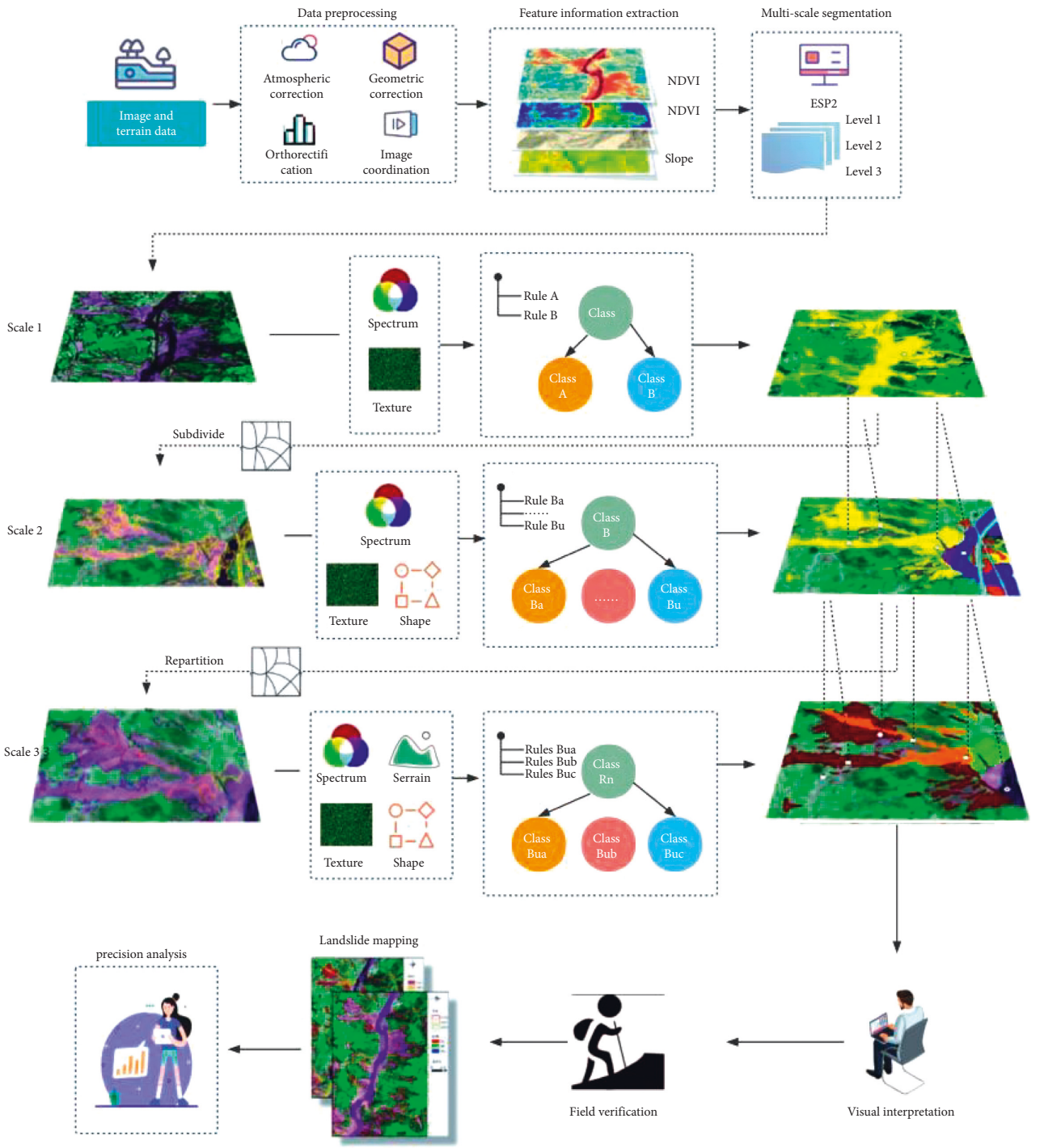

Figure 1: High-resolution remote sensing image recognition.

value, the probability of i can be expressed by the following formula:

$$p_i = \frac{H_i}{M \times N}. \tag{2}$$

In order to form a comparison with equation (2), $p_0(t)$ is used to represent the probability of class C_O, and the formula is as follows:

$$P_0(t) = \sum_{i-0}^{t} p_i, \tag{3}$$

$p_1(t)$ represents the probability generated by category C_O, and the formula is as follows:

$$P_1(t) = \sum_{i-i+1}^{L-1} P_i = 1 - P_0(t), \tag{4}$$

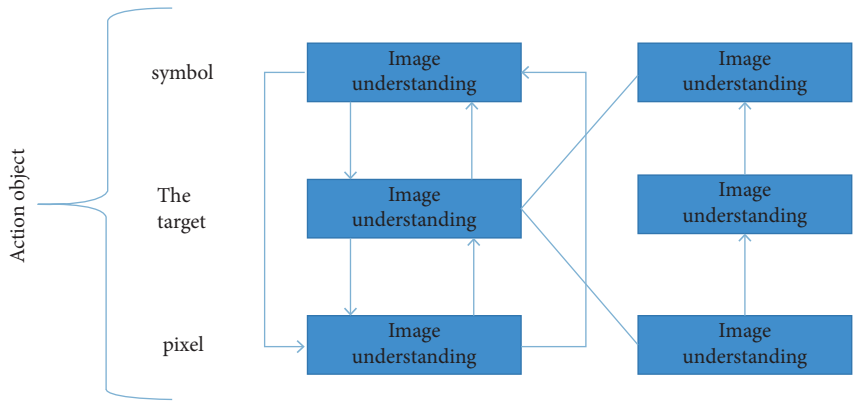

Figure 2: The position of image segmentation in image engineering.

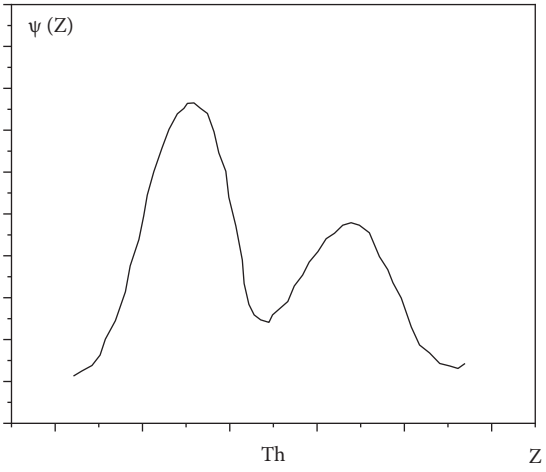

Figure 3: Threshold segmentation.

$\mu_0(t)$ represents the average gray level of pixels in the category C_O, and the formula is as follows:

$$\mu_0(t) = \sum_{t-0}^{i} \left(i \frac{p_i}{p_0(t)} \right), \tag{5}$$

$\mu_1(t)$ represents the average gray level of pixels in the category C_1, and the formula is as follows:

$$\mu_1(t) = \sum_{i-i+1}^{L-1} \left(i \frac{p_i}{p_1(t)} \right). \tag{6}$$

Then, the interclass variance $\delta_b(t)$ of the image can be calculated as shown in the following formula:

$$\delta_b(t) = P_0(t)\mu_0^2(t) + P_1(t)\mu_1^2(t). \tag{7}$$

At first, support vector machines were only used to solve two types of classification problems. In the field of experimental research, BSVM is used to represent two kinds of support vector machines, which can solve the classification problem of two kinds and obtain the structure type data with categories. However, most of the problems encountered in practical applications are multiclassification problems, so support vector machines complete the multiclassification goals through different paths. Then, in the research, BSVM can be combined to obtain the support vector of multiple classifications. The current support vector machine for multiple classification systems mainly includes two directions:

(1) The one-time solution method refers to the construction of a hyperplane between every two types of samples. The samples with a total number of class k can construct $K(K-1)/2$ BSVM, and each BSVM needs to distinguish the two categories in class K. And the two classification methods are used to construct the most potential classification function:

$$\begin{aligned} f_{st}(t) &= \omega_{st} \cdot \varphi(x) + b_s t \\ &= \sum_{i-sv} a_i^{st} y_i k(x_i, x) + b_{st}. \end{aligned} \tag{8}$$

When the value of the total number k is 4, the system diagram is shown in Figure 4.

(2) On the premise that the number of all categories is *(k)*, K kinds of BSVM can be formed by combining different categories [13].

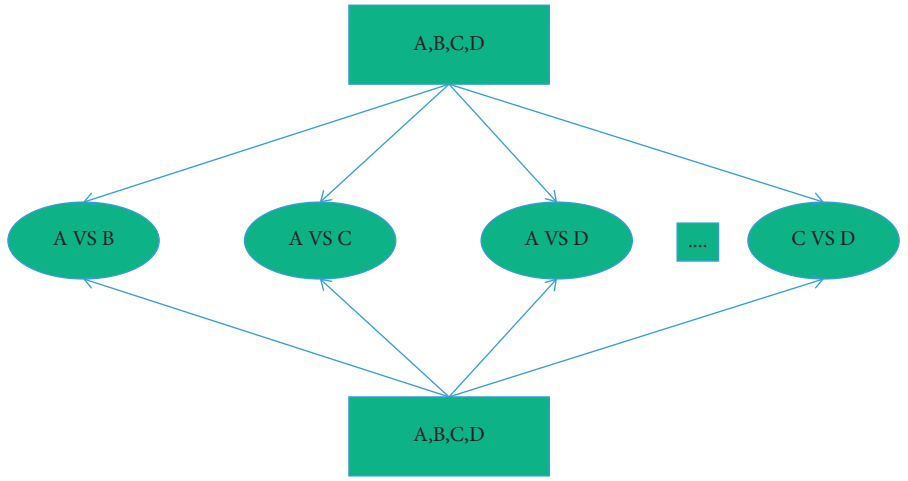

Figure 4: One-time solution method.

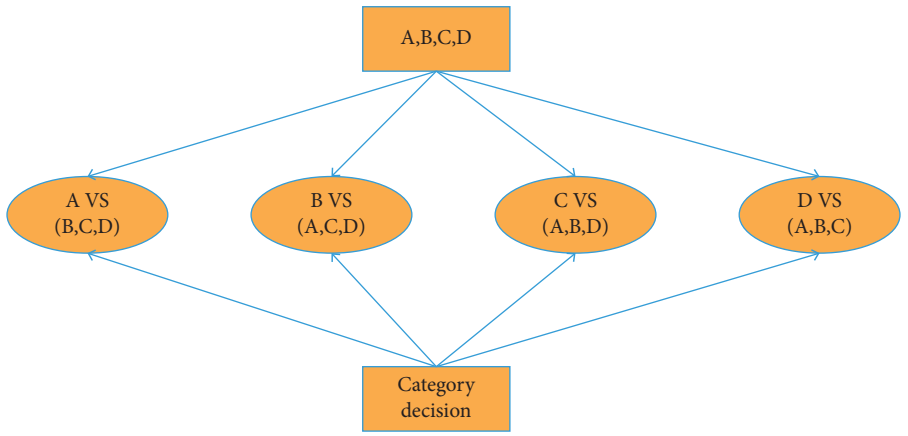

Figure 5: Multiple SVM solving methods.

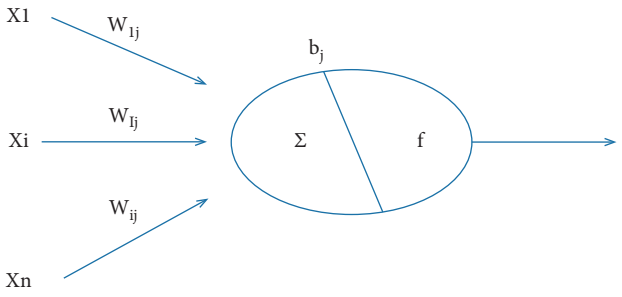

Figure 6: Neuron model.

When the value of total number k is 4, the system diagram is shown in Figure 5.

The advantage of the one-time solution method is that for each sub-SVM, because there are fewer training samples, the training time is less than that of multiple SVM, and its accuracy is also relatively high. However, its disadvantage is that when the number of classes K increases, the number of SVM will further increase, and its training time will be longer and longer.

As a multi-input single-output processing unit, the structure of the neuron itself is shown in Figure 6.

In Figure 6, n input signals are input to neuron J at the same time. w_{ij} represents the weight value of the connection between the input signal x and the neuron J, and the relationship between input and output can be expressed by the following formula:

$$y_i = f\left(b_i + \sum_{i-1}^{n}\left(x_i \times w_{ij}\right)\right). \tag{9}$$

Convolutional neural network structure, the feature space that the network can represent will also become larger, and the learning ability of the network will be strengthened [14].

3.1. Remote Sensing Classification

3.1.1. Multifeature Data. The combined use of remote sensing data and nonremote sensing data can make up for the shortcomings of single remote sensing data, play the auxiliary role of nonremote sensing data, and effectively

improve the classification accuracy of remote sensing data. The experimental area in this article is located in the west with complex terrain and large altitude differences. DEM data and slope and aspect data generated by DEM data can effectively reflect the vertical zoning of vegetation and the local growth environment, which is an effective aid to improve the accuracy of remote sensing classification. Therefore, this paper uses TM image, DEM, slope, and aspect data as the characteristic bands for classification.

3.1.2. Vegetation Zoning. According to the vegetation characteristics of arid and semiarid areas, the experiment is divided into vegetation-dominated areas and non-vegetation-dominated areas, so as to reduce the influence of the foreign matter homospectrum phenomenon in the overall classification. The normalized difference vegetation index (NDVI) is the best indicator of plant growth status and vegetation spatial distribution density and has a linear relationship with vegetation distribution density. It is a commonly used vegetation index in remote sensing estimation of vegetation coverage research. For this reason, NDVI is used for vegetation zoning. Use the preprocessed TM image to generate NDVI, statistically analyze the NDVI value of the training samples, and determine the vegetation or nonvegetation threshold NDVI = 0.18, so as to divide the experimental area into vegetation-based areas and non-vegetation-based areas [15].

The calculation method of the first-order moment of color is shown in formula (10). The first-order moment can represent the average intensity of each color component in the image.

$$\mu = \frac{1}{N}\sum_{j-1}^{N} p_{i\Delta j}. \tag{10}$$

The calculation of the second moment of color is shown in formula (11), which refers to the color variance of the image area and represents the nonuniformity of color distribution.

$$\sigma = \left(\frac{1}{N-1}\sum_{j-1}^{N}\left(P_{i,j}-\mu_i\right)^2\right)^{1/2}. \tag{11}$$

The calculation of color third-order moment is shown in formula (12), which refers to the skewness of color component and represents the asymmetry of color distribution.

$$s = \left(\frac{1}{N-1}\sum_{j-1}^{N}\left(P_{i,j}-\mu_i\right)^3\right)^{1/3}. \tag{12}$$

3.1.3. Intelligent Mining of Classification Rules. ACIOA algorithm is used to mine remote sensing classification rules for the above two regions. The algorithm takes the discrete values of each band of training samples as attribute nodes and each target class as class nodes and mines the corresponding remote sensing classification rules by searching the connection between attribute nodes and class nodes. The steps of rule mining include the following.

Before mining the classification rules, the discretization method based on information entropy is used to discretize the training sample data. In order to shorten the search time of ants, a heuristic function related to the problem is constructed to guide the search of the ant colony [16]. When the rule is constructed, the gambling wheel mechanism is used to select attribute nodes until all attributes are included in the path; then, one class node is selected and there can only be one class node, so far a complete initial classification rule is formed [17, 18]. After completing the construction of the initial classification rules, each attribute node is selected as a condition item of the rule; through rule pruning, the attribute nodes that reduce the effectiveness of the classification rules are removed, the classification rules are simplified, and the effectiveness of the classification rules is maximized. After the initial classification rule is constructed, each attribute node is selected as a condition item of the rule. Through rule pruning, remove the attribute nodes that reduce the effectiveness of classification rules, simplify classification rules, and maximize the effectiveness of classification rules.

4. Vegetation Extraction Method of High-Resolution Remote Sensing Image

Threshold segmentation is one of the most commonly used methods for remote sensing of forest vegetation. The operation steps of this method are as follows: the first step is to select indicators with obvious differences among different types, and the second step is to find out the threshold value of related indicators, so as to achieve the purpose of identifying forest vegetation cover information [19]. In the experimental research, the threshold segmentation algorithm is usually used in the research objects with a large gray difference between the extracted region and other irrelevant regions. Therefore, to achieve the best segmentation results, it should be used as a pretreatment at the beginning of the experiment.

(1) Extraction of forest vegetation by the maximum interclass method is as follows:

Step 1: Set the gray level of the used image to M, and its range is $[0, M-1]$. If the value of gray level i of the pixels contained in the image is equal, the number at this time can be expressed as N, then the total number can be expressed as e, and the probability that the value is equal to $N = N_0 + N_1 + \ldots + N_{M-1}$.

Step 2: Carry out the operation of step 1 for many times until the threshold value obtained can maximize the variance of different categories. At this time, t is the threshold value that can achieve the best segmentation effect of the image under this method.

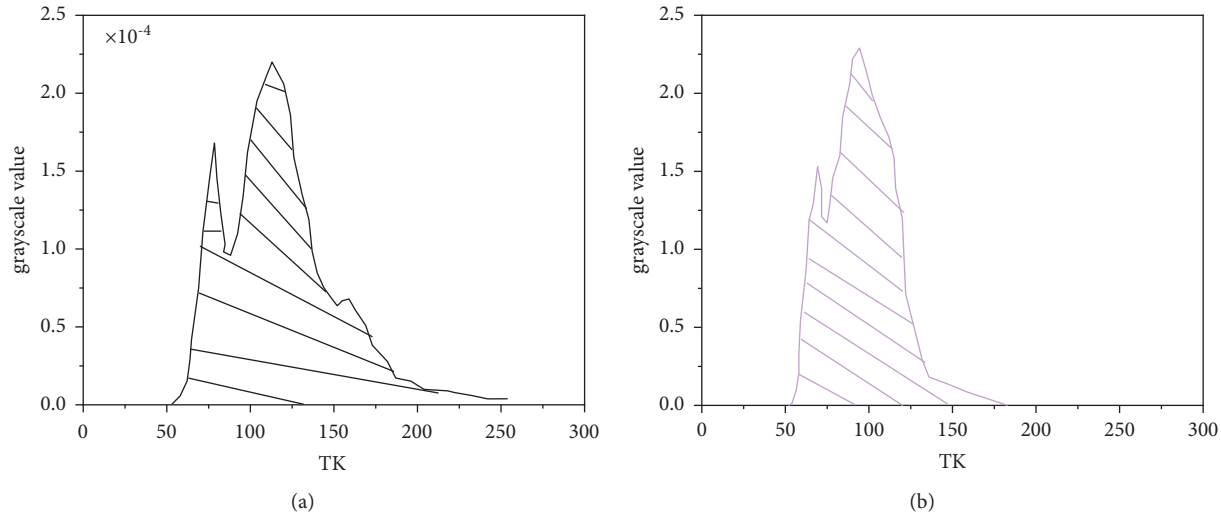

Figure 7: Gray histogram of quick bird image. (a)Histogram of experimental image 1. (b) Histogram of experimental image 2.

(2) Iterative method for forest vegetation extraction is as follows:

Step 1: First calculate the maximum gray value and minimum gray value of the image, and record them as $Z_{\max}$ and $Z_{\min}$, respectively, so that the initial value is $T_0 = (Z_{\max} + Z_{\min})/2$

Step 2: Divide the image into front and back by TK threshold, and then calculate the average gray values ZO and ZB under the two scenes respectively

Step 3: Calculate the new threshold value $TK + 1 = (ZO + ZB)/2$

The iterative method is to obtain the gray value TK through iterative calculation, so that the gray value TK can segment the remote sensing image into forest vegetation area and nonforest vegetation area [20]. The average gray value of forest vegetation area plus the average gray value of nonforest vegetation area is equal to TK. Figure 7 shows the gray histogram of the image used.

Figure 7 shows the gray histogram of two quick bird remote sensing images. The iterative method is to find a TK, TK can divide the gray histogram into two parts with equal area, and then TK is the required optimal threshold. Through experiments, it can be concluded that the optimal threshold of the experimental image a is 130 and the optimal threshold of experimental image b is 101 [21].

Combining the image segmentation effect and the two line graphs, the extraction result when $K = 4$ should be selected as the final segmentation result under the K-means algorithm (Figure 8). Therefore, in combination with the image segmentation effect and two broken line images, the extraction result when $k = 4$ should be selected as the final segmentation result under the k-means algorithm [22].

The steps of forest extraction in a fuzzy c-means clustering algorithm are not very difficult. It is a clustering algorithm that uses affiliation to determine whether each pixel of a remote sensing image belongs to a specific set. FCM is the sum of n vectors x; $x_i (i = 1, 2, \ldots, n)$ crack becomes c uncertain sets [23], and the center points of the boxes in all sets are calculated at the same time, so as to minimize the dissimilar characteristics. FCM splits a vector into an indeterminate set and, at the same time, calculates the center points of the inner boxes of all sets, so as to minimize the dissimilar characteristics. FCM distinguishes based on uncertainty. It can make the given data points fall into a certain value in the range of [0,1]. At the same time, the sum of the membership degrees of these data points is equal to 1, which can be expressed by the following formula:

$$\sum_{i=2}^{c} \mu_{ij} = 2, \quad \Delta y = 1, 2, \ldots, x. \tag{13}$$

Furthermore, the value function (objective function) of FCM can be expressed as

$$J(C, u_1, \ldots u_n) = \sum_{i-1}^{c} J_j = \sum_{i-1}^{c} \sum_{j}^{n} \mu_{ij}^{m}. \tag{14}$$

4.1. Analysis of Experimental Results. The experimental effect diagram has been shown for the experimental method used above, which can only have a general understanding of the extracted results. In order to make the experimental effect contrast more intuitive, the extraction accuracy and use time of the experimental method are compared in the form of data, as shown in Tables 1 and 2.

The experimental results in the above table show that the remote sensing images are the same, the segmentation method combining convolution neural network method, FRFCM algorithm, and Otsu and K-means algorithm is more prominent, the contour of the extracted forest vegetation area has high internal consistency, and the forest vegetation area and nonforest vegetation area have been effectively separated.

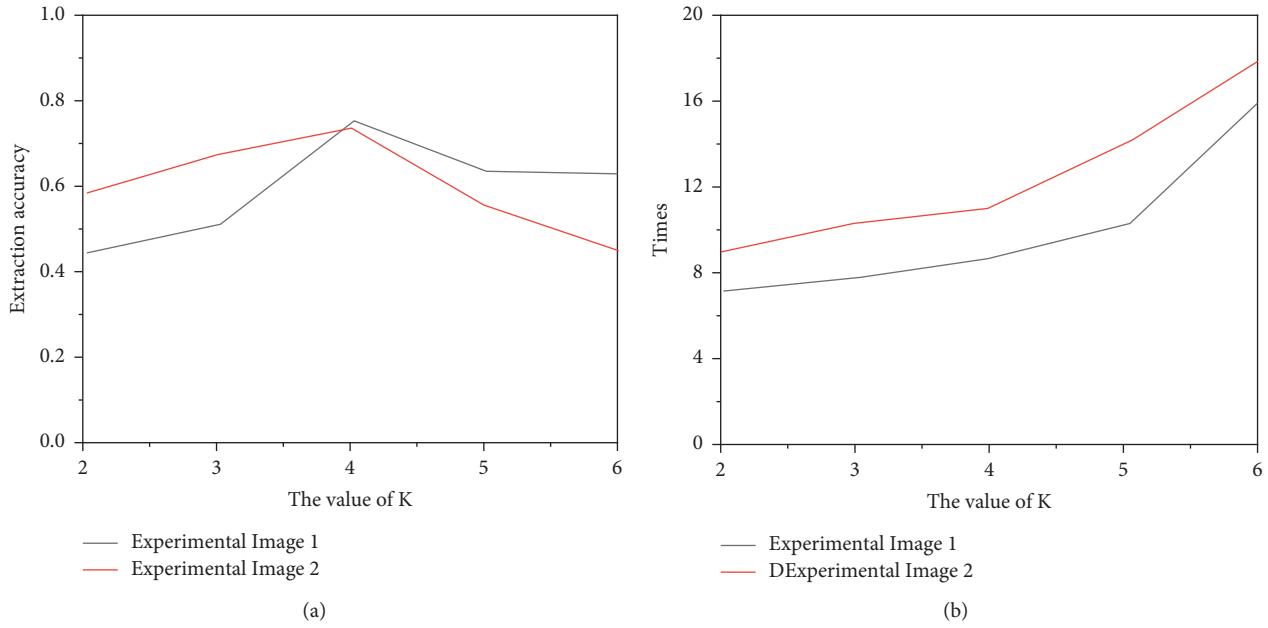

Figure 8: Extraction accuracy and time of two remote sensing images under different K values. (a)Variation of extraction accuracy with K value. (b)Variation of extraction time with K value.

Table 1: Performance comparison of experimental image 1 extraction methods.

Extraction method	Running time (s)	Extraction accuracy (%)
Maximum interclass method	6.5	75
Maximum entropy method	2.1	62
Iterative method	10.8	63
K-means algorithm	8.4	74
ISODATA algorithm	4.3	68
FCM algorithm	34.6	70
FRFCM algorithm	21.5	83
Otsu and K-means combination method	20.9	78
Convolution neural network method	13.0	90

Table 2: Performance comparison of experimental image 2 extraction methods.

Extraction method	Running time (s)	Extraction accuracy (%)
Maximum interclass method	2.1	57
Maximum entropy method	12.3	53
Iterative method	23.6	75
K-means algorithm	9.8	71
ISODATA algorithm	4.1	74
FCM algorithm	68.2	79
FRFCM algorithm	18.7	81
Otsu and K-means combination method	9.2	82
Convolution neural network method	20.4	94

In the RBF function, Y is the function setting in the kernel function, and the relationship between a and Y can be expressed by the following formula:

$$\gamma = \frac{1}{2 \cdot \sigma^2}. \tag{15}$$

By observing the data and parameter calculation images in Figure 9 and table, it can be found that the classification error rate of the two images is the lowest when they are in $C = 1$ and $\sigma = 2$, and the extraction accuracy can be obtained to be 90.62% and 91.33%, respectively. At this time, the

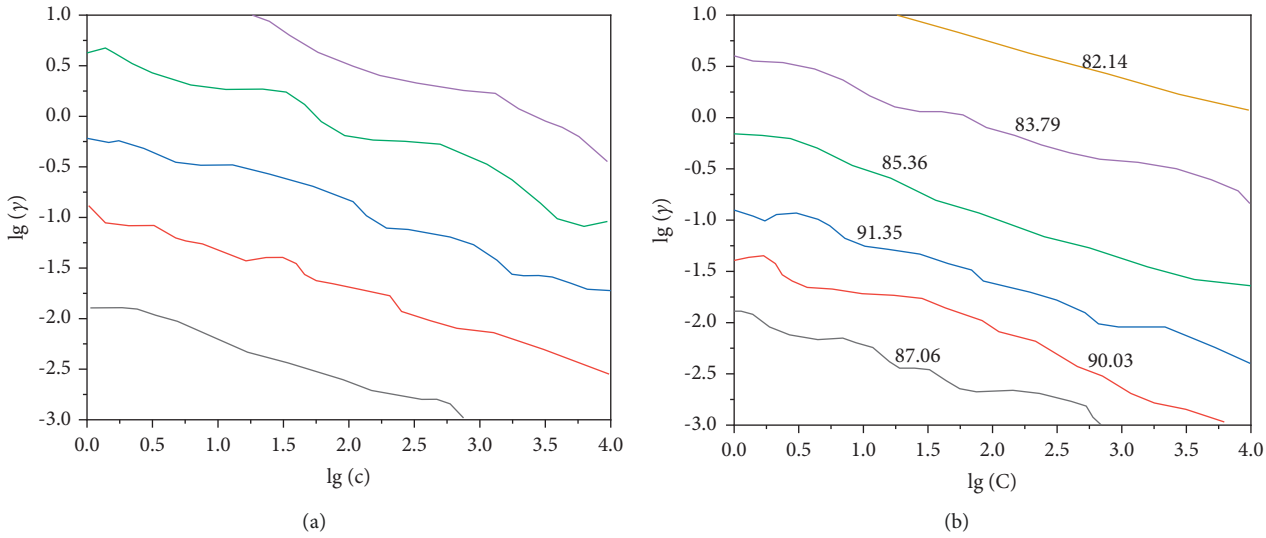

Figure 9: Calculation diagrams of optimal parameters. (a)Experimental image 1. (b) Experimental image 2.

Table 3: Comparison of running time and extraction accuracy of experimental image 1 extraction method.

Extraction method	Running time (s)	Extraction accuracy (%)
Algorithms in this chapter	9.8	90.2
FRFCM algorithm	21.5	79.3
Convolution neural network method	19.7	92.7
Otsu and K-means combination method	13.0	78.0

Table 4: Test Figure 2 comparison of extraction method running time and extraction accuracy.

Extraction method	Running time (s)	Extraction accuracy (%)
Algorithms in this chapter	10.2	91.5
FRFCM algorithm	18.9	83.0
Convolution neural network method	19.6	95.3
Otsu and K-means combination method	9.5	85.0

corresponding test time is 10.20s and 10.32s, respectively [24].

As shown in Tables 3 and 4, the running time and extraction accuracy of four extraction methods for forest vegetation area extraction of experimental image 1 and experimental image 2 are compared. It can be seen from the table that the extraction accuracy of the disturbed neural network is about 2070 higher than this group of algorithms. But the running time is nearly twice that of the algorithm in this chapter. For the "forest vegetation extraction system" developed by the forestry bureau and other departments, it is necessary to find an optimization method between high extraction accuracy and fast operation processing time, monitor the change of karst vegetation, and process the remote sensing data of dozens of GB data. Due to the large number of parameters and the long training time of the convolutional neural network model, overfitting and time-consuming are almost common problems of deep learning. Although the current deep learning methods have high accuracy, they cannot meet the requirements of fast processing of large amounts of data, which needs to be further studied. The algorithm in this chapter provides a feasible method for the development of the "Forest Vegetation Extraction System" of the Guilin Forestry Bureau, which requires high precision and fast speed, and realizes the fast and accurate processing of remote sensing big data.

5. Conclusion

Based on the synthesis of high-resolution remote sensing image target extraction research, this paper puts forward the research topic of forest vegetation target extraction based on the ecological evolution of suburban forest vegetation. The main research object of this paper is the quick bird high-resolution remote sensing images taken by satellites. Various types of image segmentation algorithms are used for experimental comparison, which provides ideas and methods for subsequent in-depth research. For the design and implementation of the forest vegetation extraction system, the methods used in this article are compiled on the Visual Studio platform, and the visual interface is designed for easy operation. Different algorithms can be compared, and the system can obtain relatively accurate forest vegetation areas.

During the experiment, because the high-resolution remote sensing image used will be affected by noise, sunlight, and other factors, the target area extracted from the image will be confused with shadow, similar or similar areas, which will make the extraction of the whole forest vegetation area difficult. There are large errors, which need to be paid attention to and improved in the follow-up research.

By looking for new algorithms or improving existing algorithms, we can obtain more information contained in remote sensing images and enrich the reference features of remote sensing image experiments, so that there will be no errors in the acquisition of training samples. This can reduce the wrong extraction and missing extraction in the forest vegetation area extraction results of high-resolution remote sensing images, and the experimental extraction results will be closer to the optimal segmentation effect [25].

Data Availability

No data were used to support this study.

Conflicts of Interest

The authors declare that there are no conflicts of interest with any financial organizations regarding the material reported in this manuscript.

Acknowledgments

This study was supported by the National Key Research and Development Program of China (No. 2021YFB3900104); the National Natural Science Foundation of China funded by the National Natural Science Foundation of China (NSFC) (Grant No. 42090014); the Qinghai Province Innovation platform construction special project of Qinghai Provincial Key Laboratory of Physical Geography and Environmental Processes (2020-ZJ-Y06); the Second Tibetan Plateau Scientific Expedition and Research Program (STEP), (Grant No. 2019QZKK0206); Key Technology R&D and Demonstration Area Construction of Carbon Neutralization Peak in Qinghai Province (2021-SF-A7-1). Study on Water Storage and Carbon Sequestration Function and Optimal Regulation of Soil-Vegetation Interface in Ecological Function Area of Southern Slope of Qilian Mountains, China (2020-ZJ-903).

References

[1] X. Sun, Q. Zhu, and Q. Qin, "A Multi-Level Convolution Pyramid Semantic Fusion Framework for High-Resolution Remote Sensing Image Scene Classification and Annotation," *IEEE Access*, vol. 9, no. 99, p. 1, 2021.

[2] A. S. Garea, D. B. Heras, and F. Argüello, "Caffe cnn-based classification of hyperspectral images on gpu," *The Journal of Supercomputing*, vol. 75, no. 3, pp. 1065–1077, 2019.

[3] Z. Jaime, Z. Jiangbin, H. Zhao, C. Qing, Z. Yang, and S. Marshall, "Novel segmented stacked autoencoder for effective dimensionality reduction and feature extraction in hyperspectral imaging," *Neurocomputing*, vol. 185, no. 12, pp. 1–10, 2016.

[4] Z. Meng, S. Chen, T. Lyu et al., "Recognition and classification of glomerular pathological images based on deep learning," *Journal of Computer-Aided Design & Computer Graphics*, vol. 33, no. 6, pp. 947–955, 2021.

[5] A. Shakya, M. Biswas, and M. Pal, "Parametric study of convolutional neural network based remote sensing image classification," *International Journal of Remote Sensing*, vol. 42, no. 7, pp. 2663–2685, 2021.

[6] G. Cao, B. Wang, H.-C. Xavier, D. Yang, and J. Southworth, "A new difference image creation method based on deep neural networks for change detection in remote-sensing images," *International Journal of Remote Sensing*, vol. 38, no. 23, pp. 7161–7175, 2017.

[7] Y. Gao, J. Shi, J. Li, and R. Wang, "Remote sensing scene classification based on high-order graph convolutional network," *European Journal of Remote Sensing*, vol. 54, no. 9, pp. 1–15, 2021.

[8] C. Chen, W. Gong, Y. Chen, and W. Li, "Learning a two-stage cnn model for multi-sized building detection in remote sensing images," *Remote Sensing Letters*, vol. 10, no. 2, pp. 103–110, 2019.

[9] Y. Wang, X. Wang, and J. Jian, "Remote sensing landslide recognition based on convolutional neural network," *Mathematical Problems in Engineering*, vol. 2019, no. 1, Article ID 8389368, 12 pages, 2019.

[10] T. Zhao, J. Xu, R. Chen, and X. Ma, "Remote sensing image segmentation based on the fuzzy deep convolutional neural network," *International Journal of Remote Sensing*, vol. 42, no. 16, pp. 6267–6286, 2021.

[11] L. Khelifi and M. Mignotte, "Deep Learning for Change Detection in Remote Sensing Images: Comprehensive Review and Meta-Analysis," *IEEE Access*, vol. 8, no. 99, p. 1, 2020.

[12] H. Hu, Z. Li, L. Li, H. Yang, and H. Zhu, "Classification of Very High-Resolution Remote Sensing Imagery Using a Fully Convolutional Network with Global and Local Context Information Enhancements," *IEEE Access*, vol. 8, no. 99, p. 1, 2020.

[13] Y. Li, L. Xu, J. Rao, L. Guo, Z. Yan, and S. Jin, "A y-net deep learning method for road segmentation using high-resolution visible remote sensing images," *Remote Sensing Letters*, vol. 10, no. 4, pp. 381–390, 2019.

[14] L. Yang and G. Cervone, "Analysis of remote sensing imagery for disaster assessment using deep learning: a case study of flooding event," *Soft Computing*, vol. 23, no. 24, pp. 13393–13408, 2019.

[15] H. Zhu, P. Zhang, L. Wang, X. Zhang, and L. Jiao, "A multiscale object detection approach for remote sensing images based on mse-densenet and the dynamic anchor assignment," *Remote Sensing Letters*, vol. 10, no. 10, pp. 959–967, 2019.

[16] X. Zhang, R. Fan, L. Ma, X. Liao, and X. Chen, "Change detection in very high-resolution images based on ensemble cnns," *International Journal of Remote Sensing*, vol. 41, no. 12, pp. 4755–4777, 2020.

[17] X. Qian, S. Lin, G. Cheng, X. Yao, H. Ren, and W. Wang, "Object detection in remote sensing images based on improved bounding box regression and multi-level features fusion," *Remote Sensing*, vol. 12, no. 1, p. 143, 2020.

[18] H. He, T. Chen, M. Chen, D. Li, and P. Cheng, "Remote sensing image super-resolution using deep-shallow cascaded convolutional neural networks," *Sensor Review*, vol. 39, no. 5, pp. 629–635, 2019.

[19] Y. Yan, Y. Zhang, and N. Su, "A Novel Data Augmentation Method for Detection of Specific Aircraft in Remote Sensing Rgb Images," *IEEE Access*, vol. 7, no. 99, p. 1, 2019.

[20] E. Puerto, J. Aguilar, R. Vargas, and J. Reyes, "An ar2p deep learning architecture for the discovery and the selection of features," *Neural Processing Letters*, vol. 50, no. 1, pp. 623–643, 2019.

[21] W. Xu, H. Liu, Q. Zhang, and P. Liu, "Response of vegetation ecosystem to climate change based on remote sensing and information entropy: a case study in the arid inland river basin of China," *Environmental Earth Sciences*, vol. 80, no. 4, pp. 1–14, 2021.

[22] H. Foroughi, A. A. Naseri, S. Boroomand Nasab et al., "A new mathematical formulation for remote sensing of soil moisture based on the red-nir space," *International Journal of Remote Sensing*, vol. 41, no. 20, pp. 8034–8047, 2020.

[23] C. Wang, W. Su, and H. Gu, "A joint change detection method on complex-valued polarimetric synthetic aperture radar images based on feature fusion and similarity learning," *International Journal of Remote Sensing*, vol. 42, no. 13, pp. 4868–4885, 2021.

[24] K. Gao, B. Liu, X. Yu, P. Zhang, X. Tan, and Y. Sun, "Small sample classification of hyperspectral image using model-agnostic meta-learning algorithm and convolutional neural network," *International Journal of Remote Sensing*, vol. 42, no. 8, pp. 3090–3122, 2021.

[25] F. Zyurt, "Efficient deep feature selection for remote sensing image recognition with fused deep learning architectures," *The Journal of Supercomputing*, vol. 76, no. 4, pp. 1–19, 2020.